Materials Letters 175 (2016) 291–295

Contents lists available at ScienceDirect

Materials Letters

journal homepage: www.elsevier.com/locate/matlet

Primary phase growth and microstructure evolution of rapidly solidifying ternary Ti-12Al-8V alloy

S.L. Wei [a], L.J. Huang [a,*], J. Chang [b], W. Zhai [b], S.J. Yang [b], L. Geng [a]

[a] School of Materials Science and Engineering, Harbin Institute of Technology, Harbin 150001, China
[b] Department of Applied Physics, Northwestern Polytechnical University, Xi'an 710072, China

ARTICLE INFO

Article history:
Received 23 February 2016
Received in revised form
15 March 2016
Accepted 3 April 2016
Available online 7 April 2016

Keywords:
Titanium alloy
Solidification
Microstructure
Crystal growth
Thermal analysis

ABSTRACT

Liquid Ti-12Al-8V alloy was rapidly solidified by electromagnetic levitation and drop tube techniques. The levitation processing avoided the violent heterogeneous nucleation of primary β phase and led to an actual maximum undercooling of 212 K ($0.11T_L$). The primary β dendrites exhibited a high growth velocity up to 14.9 m/s but subsequently transformed into basket weave structures. Drop tube experiments indicated that the final microstructure morphology was determined by the coupled influences of undercooling extent and cooling rate. If the cooling rate exceeded 3.31×10^3 K/s, the primary β phase was retained metastably to ambient temperature.

1. Introduction

Ternary Ti-Al-V system forms the basis of numerous high-performance titanium alloys widely applied in aerospace industry and chemical engineering [1–3]. Although the subsequent plastic deformation and heat treatment are the crucial procedures to produce advanced Ti-based alloys [1,4], it is equally essential to control their initial solidification process for optimizing desirable microstructures [5]. Indeed there are extensive investigations on their directional solidification [6] and rapid solidification [2,7,8] characteristics. But the underlying kinetic mechanisms of phase selection and structure evolution are still far from being completely understood. In particular, much work remains to be done about the high undercooling and dendritic growth of liquid titanium alloys. The technical barrier arises mainly from the very strong chemical reactivity of molten titanium at elevated temperatures. Nowadays, the containerless processing by electromagnetic levitation [2,9] and drop tube [10,11] techniques may provide an effective access to solve such a challenge.

The dendrite growth of primary crystalline phase usually dominates the rapid solidification process of undercooled liquid alloys [12–15]. Both the structural morphology and solute distribution, which determine the applied properties of solidified alloys, depend upon the growth kinetics of primary phases. Therefore, the quantitative measurement of dendritic growth velocity versus liquid alloy undercooling is a vital step to explore the rapid solidification mechanisms of titanium alloys. Another controlling factor is the cooling rate of alloy melt during solidification, which represents the time-dependent feature of crystallization kinetics. The objective of this work is to investigate the liquid state undercoolability and primary dendrite growth of ternary Ti-12 wt%Al-8 wt%V alloy by both electromagnetic levitation and drop tube techniques. A comparative study of bulk undercooled alloy melt with rapidly cooled alloy droplet may shed a bit more light on the microstructural evolution mechanisms of titanium alloys.

2. Materials and methods

Ternary Ti-12 wt%Al-8 wt%V (equivalent to $Ti_{73.5}Al_{19.6}V_{6.9}$ in atomic fraction) master alloy was prepared with ultrahigh vacuum arc melting furnace from 99.99% pure Ti, 99.999% pure Al and 99.8% pure V. Its liquidus temperature was determined as 1905 K by measuring the heating and cooling curves of inductively melted 10 g sample with a W-Re5/26 thermocouple. The electromagnetic levitation apparatus was equipped with a 200 kHz and 30 kW power source and a Raytek Marathon MRIS infrared pyrometer. It was firstly evacuated to 10^{-5} Pa and then backfilled with Ar gas to 1 atm. Each levitated sample with 6–8 mm diameter was superheated to 300–500 K above the liquidus temperature and cooled

* Corresponding author.
E-mail address: huanglujun@hit.edu.cn (L.J. Huang).

http://dx.doi.org/10.1016/j.matlet.2016.04.043
0167-577X/

down by a flow of He gas refrigerated in liquid nitrogen. In order to experimentally determine the dendrite growth velocity of primary β phase, the infrared pyrometer device was applied to monitor the specimen temperature; meanwhile a photoelectric detector was used to measure the recalescence time. The 3 m drop tube with 150 mm inner diameter, attained a vacuum of 5×10^{-5} Pa. It provided a free-fall time period of 0.78 s and a reduced gravity level of $10^{-3}-10^{-6}$ g_0. For each experiment, a sum of 1–3 g master alloy was contained inside a 13 mm ID × 15 mm OD × 160 mm quartz tube with a 0.2 mm diameter orifice at its bottom. The bulk alloy was melted by induction heating, superheated to 100 K above its liquidus temperature and finally atomized by a high-pressure ejecting gas into a great number of freely falling droplets. After experiments, all the samples were analyzed according to standard metallographic procedure with an aqueous etchant of HF+HNO_3. An FEI Sirion 200 scanning electron microscope and an INCA 300 energy dispersive spectrometer were applied to investigate their phase constitution and microstructural morphology.

3. Results and discussion

3.1. Bulk undercooling at levitated state

As shown in Fig. 1(a), ternary Ti-12Al-8V alloy is located at the Ti-rich corner of Ti-Al-V phase diagram [3]. Under equilibrium conditions, its solidification process is dominated by the nucleation and growth of primary β-Ti solid solution phase, which has a BCC (body centered cubic) structure and dissolves both Al and V solutes. Because titanium involves a polymorphic transformation at solid state, the primary β-Ti phase usually transfers into HCP (hexagonal close packed) structured α-Ti phase as long as the cooling rate is not extremely high.

When a bulk sample of Ti-12Al-8V alloy was melted and solidified at levitated state, the elimination of crucible and mould walls minimized the chances to induce the heterogeneous nucleation of β phase. Furthermore, the ultrahigh vacuum plus Ar filling ensured an efficient protecting atmosphere for the alloy melt to avoid oxidation. Thus a maximum undercooling of ΔT=212 K (0.11T_L) has been achieved experimentally by this alloy, as shown in Fig. 1. The levitation experiments also revealed that a superheating of at least 300 K above its liquidus temperature was necessary to obtain a significant undercooling. A higher degree of superheating favors the enhancement of alloy melt undercooling in two respects. At first, the potential heterogeneous nuclei formed by the inherent impurities of master alloy may be either melted or passivated at sufficiently high temperatures. Secondly, the atomic cluster size inside the liquid alloy is reduced so that the evolution of homogenous nuclei is hindered to a certain extent.

Once a crystalline nucleus of β phase forms in the undercooled liquid Ti-12Al-8V alloy, the negative temperature gradient in front of solid-liquid interface drives it to grow rapidly in dendritic mode. Fig. 1(b) presents the measured dendrite growth velocity V of primary β phase versus alloy melt undercooling ΔT. Evidently, β phase dendrites attained a maximum growth velocity of 14.9 m/s at 212 K undercooling. The statistical fitting analysis of experimental data revealed a power function relation as below:

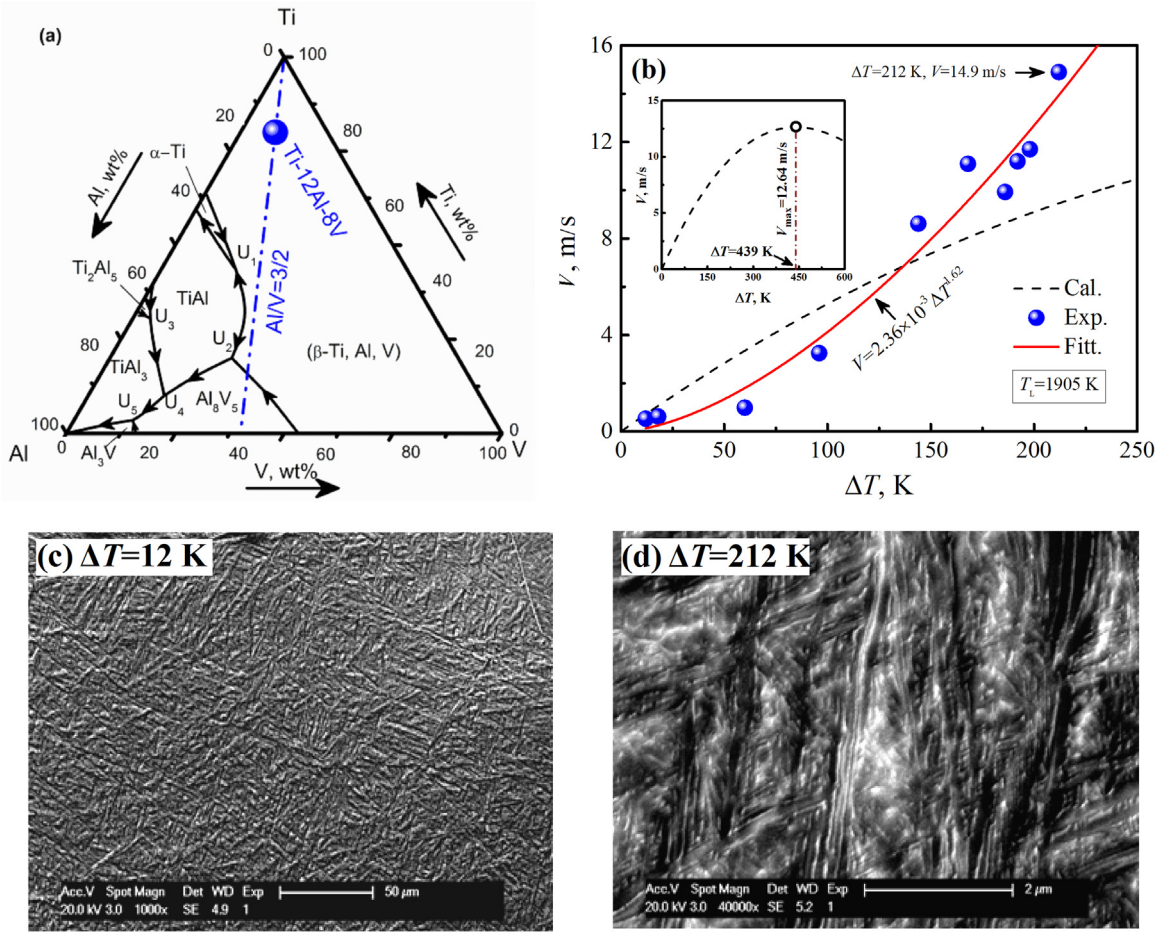

Fig. 1. Dendritic growth of primary β phase in undercooled Ti-12Al-8V alloy at levitated state: (a) alloy composition selection in ternary Ti-Al-V phase diagram, (b) measured and calculated dendritic growth velocity, (c) microstructure at 12 K undercooling and (d) microstructure at 212 K undercooling.

Table 1
Physical parameters of Ti-12Al-8V alloy.

Physical parameter	Unit	Value
liquidus temperature T_L	K	1905
diffusion activation energy Q	J	7.5×10^{20}
latent heat ΔH_m	J/mol	1.61×10^4
molar volume V_m	m^3/mol	1.09×10^{-5}
interface atom number n_L	$1/m^2$	1.085×10^{19}
atom vibration frequency f_a	Hz	2×10^{13}
attachment probability P_a	–	0.5
liquid density ρ_L	kg/m^3	4.03×10^3
liquid specific heat C_{PL}	J/kg · K	752.4
liquid emissivity ε_L	–	0.45

$$V = 2.36 \times 10^{-3}\Delta T^{1.62} \quad (1)$$

So far, a practical analytical model to describe the dendritic growth in undercooled ternary or multicomponent alloys is still in lack. To a first order approximation, the continuous growth model of crystalline solid [16] which originated from Jackson's classic analysis [17] is drawn here to conduct a preliminary comparison:

$$V = \frac{P_a n_L f_a V_m}{N_A}\exp\left(-\frac{Q}{k_B T}\right)\left[1 - \exp\left(-\frac{\Delta G_{LS}}{k_B T}\right)\right] \quad (2)$$

in which V and T are the crystal growth velocity and the liquid alloy temperature. The definitions and values of other physical parameters are listed in Table 1. The dashed line in Fig. 1 (b) illustrates the calculated results of Eq. (2). Obviously, this represents a quite different variation trend for the dendritic growth velocity of primary β phase if compared with the experimental measurements. The reasonable aspect of Eq. (2) lies in that it predicts a critical undercooling of 439 K ($0.23T_L$) beyond which the β phase dendrites might show decreasing growth velocity. But the correspondingly predicted maximum dendrite growth velocity is only 12.64 m/s, which is even lower than the experimentally detected maximum value of 14.9 m/s at 212 K (0.11 T_L) undercooling.

Since the sample cooling rate was only 50–100 K/s at levitated state, the primary β phase experienced the solid state transformation into HCP structured α-Ti phase after the rapid solidification of Ti-12Al-8V alloy. The ambient temperature microstructures are shown in Fig. 1(c) and (d). At the small undercooling of 12 K, basket weave structures were formed inside the whole sample. This type of microstructure became continually refined as alloy undercooling increased up to 212 K. It is noticeable in Fig. 1(d) that the interlamellar spacings were reduced to submicron or even nanoscale size.

3.2. Rapid solidification at microgravity state

During drop tube experiments, bulk Ti-12Al-8V alloy melt was initially atomized into small droplets with diameters of 84–1810 μm. It is presently not practical to directly measure the cooling curve of individual alloy droplet. Considering the small size of these droplets, it is rational to neglect their internal temperature gradients. For each freely falling alloy droplet within Ar gas atmosphere, the heat transfer process is mainly controlled by radiation and convection. Consequently its cooling rate R_c before the occurrence of solidification can be derived from the following coupled equations [18]:

$$R_c = \frac{6}{\rho_L C_{PL} D}\left[\varepsilon_L \sigma_{SB}(T^4 - T_0^4) + h(T - T_0)\right] \quad (3)$$

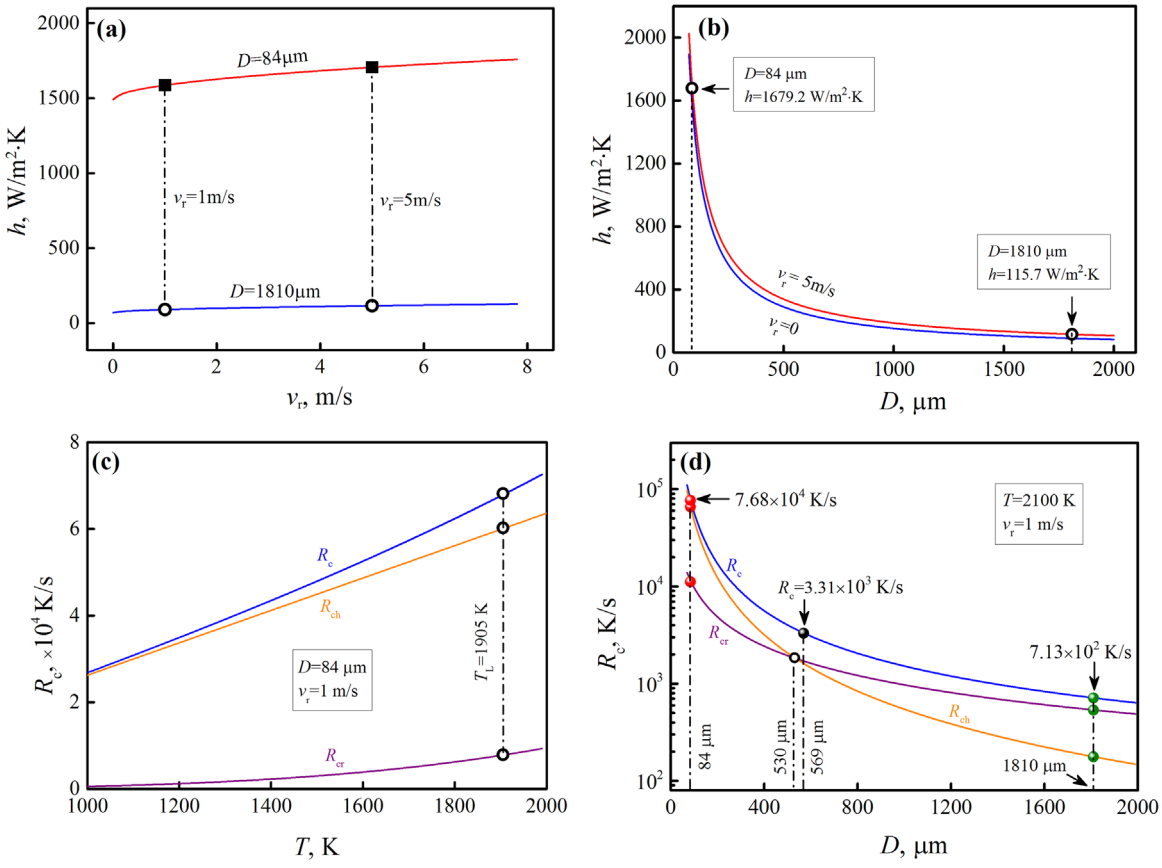

Fig. 2. Heat transfer characteristics of Ti-12Al-8V alloy droplets inside drop tube: (a) and (b) calculated convective heat transfer coefficients, (c) and (d) calculated cooling rates.

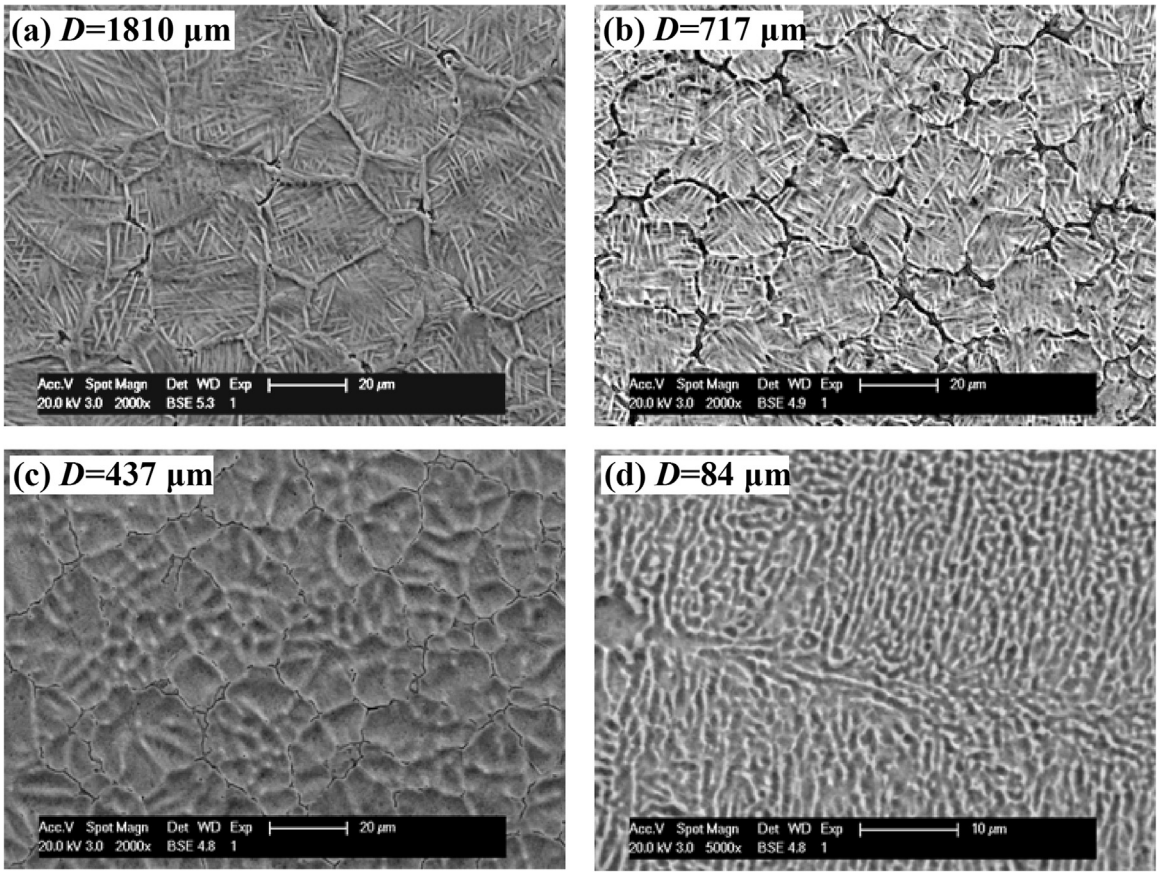

Fig. 3. Rapidly solidified microstructures of Ti-12Al-8V alloy versus droplet diameter: (a) and (b) basket weave structures of large droplets, (c) and (d) metastable primary β dendrites of small droplets.

$$h = \frac{\lambda_0}{D}\left[2 + 0.6\left(\frac{\rho_0 v_r D}{\eta_0}\right)^{1/2}\left(\frac{\eta_0 C_{P0}}{\lambda_0}\right)^{1/3}\right] \quad (4)$$

where D, v_r and h are the droplet diameter, moving velocity and convective heat transfer coefficient, respectively. In contrast, T_0, λ_0, ρ_0, C_{P0} and η_0 represent the temperature, thermal conductivity, density, specific heat and viscosity of surrounding gas. Table 1 gives the physical parameters used for calculations.

The first term of Eq. (3) describes the cooling rate R_{cr} by thermal radiation, while the second one is the cooling rate R_{ch} depending on thermal convection. Fig. 2(a) and (b) demonstrate that the convective heat transfer coefficient h is very sensitive to alloy droplet diameter D, but increases only slightly with the rise of falling velocity v_r. For a constant falling velocity, the h value of the small 84 μm droplet is more than one order of magnitude larger than that of the large 1810 μm droplet. The theoretically calculated cooling rates of Ti-12Al-8V alloy droplets are provided in Fig. 2 (c) and (d). For a specific droplet diameter, its cooling rate decreases significantly with the descending of temperature. At any temperature, the droplet cooling rate always increases rapidly with the reduction of its diameter. At the initial temperature of 2100 K, Fig. 2(d) shows that the smallest 84 μm droplet attains a cooling rate as high as 7.68×10^4 K/s, whereas the cooling rate of the largest 1810 μm droplet is only 7.13×10^2 K/s. There appears a theoretical 530 μm threshold for the droplet diameters. For those smaller alloy droplets of diameter $D < 530$ μm, $R_{ch} > R_{cr}$, this means that thermal convection is the dominant mechanism for heat dissipation. In the case of larger alloy droplets with $D > 530$ μm, $R_{cr} > R_{ch}$, the cooling mechanism relies mainly on thermal radiation.

Fig. 3 shows the two typical kinds of ambient temperature microstructures for the rapidly solidified alloy droplets. A statistical survey of the structural morphologies for several hundreds of alloy droplets reveals that primary β phase dendrites transformed into the basket weave structures shown in Fig. 3(a) and (b), if droplet diameters were larger than 569 μm. On the other hand, Fig. 3(c) and (d) demonstrate that those small alloy droplets with diameters below 569 μm were able to retain the primary β dendrites unto ambient temperature. By referring to Fig. 2(d), it is evident that the critical cooling rate to suppress the polymorphic transformation of primary β phase is at least 3.31×10^3 K/s. This is one to two orders of magnitude higher than the actual cooling rate of electromagnetically levitated bulk alloy samples. Thus there is no wonder that all the levitation experiments only resulted in the transformed basket weave microstructures shown in Fig. 1.

4. Conclusions

In summary, electromagnetic levitation can effectively prevent the violent heterogeneous nucleation of liquid Ti-12Al-8V alloy. As a result, the bulk alloy melt has attained a high undercooling of 212 K ($0.11T_L$) experimentally at levitated state. Primary β-Ti phase displayed a rapid dendritic growth velocity up to 14.9 m/s and transformed into basket weave structures after solidification. Experimental measurements revealed a power function relation of dendritic growth velocity versus alloy undercooling, which differs significantly from the theoretical predication of continuous growth model for crystalline solids. It was found by drop tube

experiments that the critical cooling rate to suppress the polymorphic transformation of primary β phase was 3.31×10^3 K/s, below which basket weave structures were always formed. This demonstrates that the final microstructure morphology of ternary Ti-12Al-8V alloy depends upon the coupled influences of both liquid undercooling and cooling rate.

Acknowledgements

The authors are very grateful to Dr. K. Zhou, Dr. S.W. Tang, Dr. X. P. Cui, Ms. Y. Jiao, Mr. Y. H. Wu and Assoc. Prof. L. Hu for their enthusiastic help with the experiments and critical discussion on the calculation results. This work was financially supported by National Natural Science Foundation of China (Nos: 51471063, 51271064, 51401167, and 51571164).

References

[1] L.J. Huang, L. Geng, H.X. Peng, Microstructurally inhomogeneous composites: is a homogeneous reinforcement distribution optimal? Prog. Mater. Sci. 71 (2015) 93–168.
[2] O. Shuleshova, T.G. Woodcock, H.G. Lindenkreuz, R. Hermann, W. Loeser, B. Buchner, Metastable phase transformation in Ti-Al-Nb undercooled melts, Acta Mater. 55 (2007) 681–689.
[3] H. Wang, N. Warnken, R.C. Reed, Thermodynamic and kinetic modeling of bcc phase in the Ti-Al-V ternay system, Mater. Sci. Eng. A 528 (2010) 622–630.
[4] E. Brandl, D. Greitemeier, Microstructure of additive layer manufactured Ti-6Al-4V after exceptional post heat treatments, Mater. Lett. 81 (2012) 84–87.
[5] C.D. Anderson, W.H. Hofmeister, R.J. Bayuzick, Solidification kinetics and metastable phase formation in binary Ti-Al, Metall. Trans. 23A (1992) 2699–2714.
[6] R. Srinirasan, S. Tarnirisakandala, Influence of trace boron addition on the directional solidification characteristics of Ti-6Al-4V, Scr. Mater 63 (2010) 1244–1247.
[7] Y.C. Liu, Lamellar spacing and mechanical properties of undercooled Ti-45Al-2Cr-2Nb alloy, Mater. Lett. 57 (2003) 2262–2266.
[8] O. Shuleshova, D. Holland-Moritz, A. Voss, W. Loeser, In situ observation of solidification in Ti-Al-Ta alloys by synchrotron radiation, Intermetallics 19 (2011) 688–692.
[9] N. Wang, B. Wei, Thermodynamic properties of highly undercooled liquid TiAl alloy, Appl. Phys. Lett. 80 (2002) 3515–3517.
[10] Z.C. Xia, W.L. Wang, S.B. Luo, B. Wei, Liquid phase separation and rapid dendritic growth of highly undercooled ternary $Fe_{62.5}Cu_{27.5}Sn_{10}$ alloy, J. Appl. Phys. 117 (2015) 054901-1–054901-8.
[11] S. Kano, Y. Matsumura, H. Uchida, $TbFe_2$ giant magnetostrivtive alloy prepared by drop tube system, J. Alloy. Compd. 408–412 (2006) 331–334.
[12] W.L. Chan, R.S. Averback, D.G. Cahill, Y. Ashkenazy, Solidification velocity in deeply undercooled silver, Phys. Rev. Lett. 102 (2009) 095701-1–095701-4.
[13] J. Chang, H.P. Wang, K. Zhou, B. Wei, Rapid solidification and solute trapping within undercooled ternary Ni-5%Cu-5%Mo alloy, Appl. Phys. A 19 (2012) 139–143.
[14] M. Mullis, Prediction of the operating point of dendrites growing under coupled thermosolutal control at high growth velocity, Phys. Rev. E 83 (2011) 061601-1–061601-9 061601-1-9.
[15] S. Griesser, C. Bernhard, R. Dippenarr, Effect of nucleation undercooling on the kinetics and mechanism of the peritectic phase transition steel, Acta Mater. 81 (2014) 111–120.
[16] Y.N. Yu, Principles of Physical Metallurgy, Metallurgical Industry Press, China 2000, pp. 229–234.
[17] W. Kurz, D.J. Fisher, Fundamentals of Solidification, 4th edition, Trans Tech Publications Ltd, Switzerland 1998, pp. 216–219.
[18] K. Wu, Transport Principles of Metallurgical Process, Metallurgical Industry Press, China 2011, pp. 169–178.